Robotica (2012) volume 30, pp. 279–287. © Cambridge University Press 2011
doi:10.1017/S0263574711000579

Analysis, simulation, and implementation of a human-inspired pole climbing robot

A. Sadeghi, H. Moradi* and M. Nili Ahmadabadi

Robotics and Artificial Intelligence Laboratory, Control and Intelligent Processing Center of Excellence, School of Electrical and Computer Engineering, College of Engineering, University of Tehran, Room 709, North Kargar St. Tehran, Iran 14395-515

(Received in Final Form: May 12, 2011; accepted May 10, 2011. First published online: June 15, 2011)

SUMMARY

In this paper, we present the design, static analysis, simulation, and implementation of a novel design for a naturally stable climbing robot that has been inspired from human pole/tree climbers. The other benefits of this robot, besides being naturally stable, are its simple design, ease of control, light weight, simple mechanism, and fast climbing speed. The robot consists of three wheels, two free and one active wheel, which enable the robot to climb or descend poles. The free wheels are almost frictionless, while the active wheel has enough friction to be able to apply force on the pole for stable climbing or descending. The wheels are designed in V-shape such that the robot can compensate for misplacements eliminating possible detachment from poles. Although the robot can operate with a single free wheel, however, an extra free wheel is added to increase the stability and safety of the robot. In this paper, the static analysis of the robot is presented and the robot is simulated. Furthermore, the robot is actually implemented and successfully tested in two sizes, a small size and a big/full size. The full-scale prototype has been equipped with washing and inspection tools and tested washing actual street lights. The results show the unique characteristics of this robot that make it more stable if more weight is carried.

KEYWORDS: Design; Service robots; Novel applications of robotics; Teleoperation; Biomimetic robots; Pole climbing robots.

1. Introduction

While climbing ability was needed to escape animals or collect fruits from trees in early days of human existence, it has become a necessity in the era of technology. In other words, climbing poles to access power transmission lines, telephone lines, and lamps have been routine tasks for technicians and municipal workers (Fig. 1a). Unfortunately, climbing poles can be dangerous and needs expertise to avoid injuries or loss of lives. Although it is possible to use lifts to provide easy access to the end of poles (Fig. 1b), however, this is not always easy or practical due to unavailability of adequately large lifts (some poles are about 18 m tall). Furthermore, this approach is dangerous on highways in which a lift needs to operate on high-speed lanes. In addition, it creates traffic jams and congestions due to blocking the high-speed lane. Finally, the operation of the lifts would be greatly affected by weather since operation in a slightly windy weather can be dangerous, especially for large lifts.

Consequently, there have been many efforts to design robots, either teleoperated or autonomous ones, to climb poles. Unfortunately, the majority of these robots have limited payload, and become unstable or fall if the payload is increased. Furthermore, complexity of climbing mechanisms, low climbing speeds, or requiring sophisticated control systems are other major drawbacks of the majority of existing climbing robots.

In this paper, we present a robotic pole/tree climber that can be used for moving up light poles, telephone line poles, or similar vertical structures or trees for the purpose of cleaning, maintenance, or inspection. The proposed design is inspired from human climbers, which use a strap and their weight to stably and consistently climb poles. The major advantage of this design is in its capability of carrying high payloads, and its natural stability. Furthermore, it has a simple design, a light structure, simple mechanism, and fast climbing speed in addition to a simple controller.

2. Related Work

Climbing robots have been under investigation for the last 20 years, mainly due to the need for inspections, cleaning, and maintenance of high rises,[1,2] fuel and water tanks,[5] nuclear facilities,[4] poles,[3] and pipes.[4] Almost all designs use one of the following five methods to hold and climb walls or poles: (a) vacuum suction cups, (b) magnetic hand, (c) adhesive materials, (d) grippers, and (e) wheels or legs. Using vacuum suction cups[14–16] has been the dominant method selected by many researchers. The robot can stick to a surface where adequate suction cups are placed on flat surfaces and vacuum is created. Unfortunately, this method has not been successful for widespread use because adequate a vacuum cannot be generated on rough surfaces, especially on poles and trees with round or rough surfaces. Furthermore, such a robot is not naturally stable and would fall if the vacuum mechanism fails or stops working. Finally, the payload of such a system is limited due to its dependence on the number and size of suction cups.

Bonaccorso *et al.*[10] used a new generation of the suction cups, called VORTEX suction cups initiated from Duke University that worked on nonsmooth surfaces, such as

* Corresponding author. E-mail: moradih@ut.ac.ir

https://doi.org/10.1017/S0263574711000579 Published online by Cambridge University Press

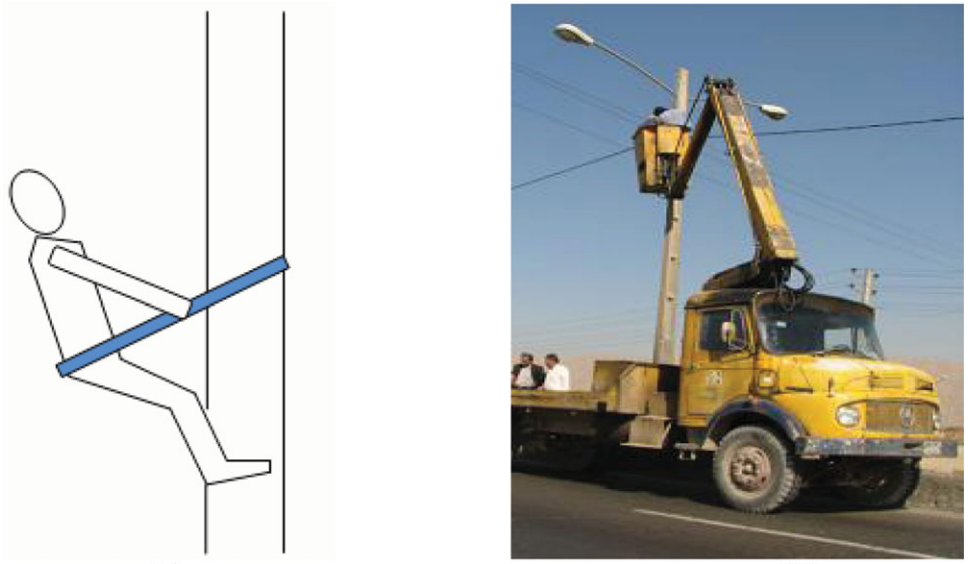


Fig. 1. (Colour online) (a) A human pole climber using climbing straps to provide support. (b) A heavy lift is used for lifting a person up to a lamp post for cleaning or fixing purposes.

concrete surfaces. A high-speed fan at the middle of a rigid plastic cup generates a vortex that creates a strong adhesion force. The results are promising in eliminating the need for very smooth surfaces for successful suctioning action. Moreover, this new mechanism allows sliding motion of the suction cup on the surface and allows passing over small obstacles on the surface. However, this mechanism needs a minimal flat surface to provide adequate suctioning result. Consequently, this approach is not suitable for poles, which are normally round or with very small flat surfaces. It should be mentioned that nonflat surfaces may be usable on poles to use VORTEX suction cups and create adhesion force. However, due to change in the size of poles, this mechanism would not be useful. Finally, the limited payload is still a shortcoming for this mechanism.

There are few examples using magnets[12,13] for climbing fuel tanks. Since magnets only work on metallic walls and surfaces, this limits the use of these robots. Also, this mechanism has the same limits as suction cup mechanism, such as having limited payload and not being fail-safe. In other words, to carry large payloads, the robot needs stronger magnet resulting in bigger and heavier mechanism. In addition, if the magnetic part fails or its power gets disrupted, the robot looses the contact with the surface and falls.

The adhesive materials and Gecko-like robots[3] are the new generation of the climbers, which are inspired by biology. Although these types of robots may be useful in the future, the current technology provides limited payload for the robots using these mechanisms. Thus, these robots are not suitable for jobs with high payload. Furthermore, the sticking mechanisms, either the adhesive-type or Gecko-type, are not suitable for operation in dirty and dusty environments. It is important to mention that the Gecko-type robots have noticeable climbing speed that makes them appropriate for climbing tall structures.

The gripper-based robotic climbers use grippers to hold poles or trees.[9,17,18] In other words, actuators or springs are needed to press the robot against a pole to overcome the weight of the robot by using friction force. Thus, the friction force would be proportional to the force applied by the actuators or springs. Consequently, the robot cannot handle large payloads unless stronger actuators or springs are used. Furthermore, a gripper-based robot need a mechanism to prevent free fall of a robot if the control system fails, or the power gets disrupted. Otherwise, the robot may not be safe enough to be used in urban environments and can be dangerous to its operators. The complexity of the gripper mechanism and its control are other disadvantages of this class of climbers.[11]

Degani *et al.*[8] proposed an innovative approach based on dynamic motion of a single actuated mechanism that can climb or descend pipes. Although this is an innovative approach in climbing, it is limited to small systems and may not carry heavy payloads. Furthermore, its nonsmooth motion is not desirable for pole climbing for the purposes of inspection and cleaning.

Finally, the wheel or leg-based robots work when the robot is inside a pipe type pole/tunnel, or the robot can fully embrace the pole/pipe from outside.[3,6,7,11] The wheel-based robots have the advantage of moving smoother on poles or trees than the leg-based robots. Furthermore, they normally have good climbing speed. However, both mechanisms suffer from limited payload similar to the robots that grab poles or trees.

There are very specific pole climbing robots, such as the snake robots that wrap around poles to climb.[19,20] Such a design suffers from the same issue as the others, i.e., the limited payload. As mentioned earlier, the main issue, in all of these designs, except UT-PCRI[4] and Pobot V2,[21] is the limitation on their payload, i.e., the higher the payload, the harder it is to design a stable robot. In many cases, it would be impossible to design a stable robot with high payloads. Furthermore, the design and control complexity is another issue for these robots. Finally, a reliable climbing robot needs to be stable even in case of power failure, like UT-PCRI.

https://doi.org/10.1017/S0263574711000579 Published online by Cambridge University Press

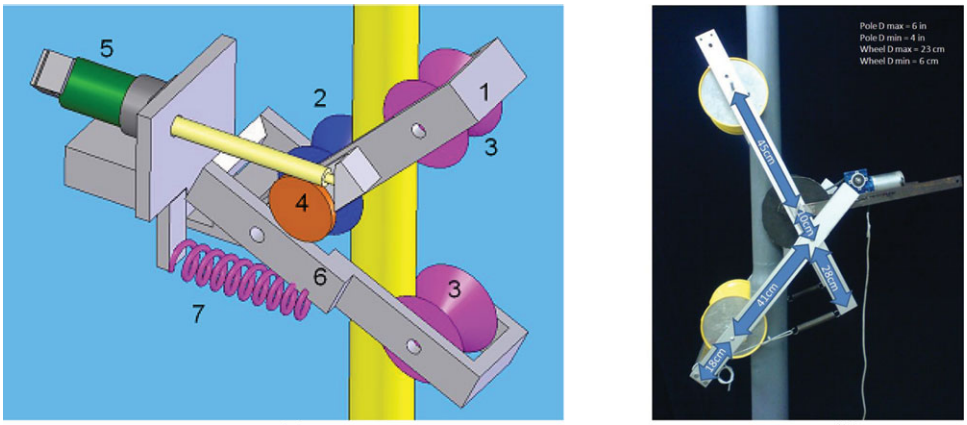


Fig. 2. (Colour online) The human-inspired pole climbing robot. (a) It consists of the SA (1), the active wheel (2), the passive wheels (3), the worm gearbox (4), the motor (5), the SL (6), and the safety spring (7). The active wheel is placed on the strap arm. (b) The dimensions of the full-scale implementation.

However, almost all of the above robots are not fail-safe and fall in case of power disruption.

In this paper, we present a robotic pole climber, i.e., UT-PCRII, with a special characteristic: the heavier the payload, the better the stability of the robot. In contrast to the majority of the pole climbing robots, the proposed design uses the payload to create the friction force. Thus, the higher the payload would result to higher friction force, i.e., a natural and automatic compensation for the increased payload is implemented in the system. We even show that the stability becomes independent of the weight if the friction is higher than a certain amount. Furthermore, the V-shape wheels provide a natural defense mechanism against rotations around poles. Also the V-shape wheels force the robot to align with poles. Finally, a mechanism is implemented to increase the stability of the robot, especially when the robot moves from a high-diameter section of the pole to a low-diameter section in which the amount of friction force drops. This safety mechanism, which is called the spring leg, also helps the robot to regrasp a pole in case of free falls.

The simple mechanism, fast climbing speed, ease of control, independence from the poles' surface material, and light weight are other features of this robot. This design is inspired from the human-climber's action, which relies on a strap around his waist (Fig. 1a) to provide enough force on his foot to stick to the pole. A climber may push his waist back to provide more torque around his waist to create more force on the contact point, i.e., his foot.

It should be mentioned that Fauroux and Morillon[21] proposed a rolling self-locking mechanism that uses the weight of the robot to stick to a pole, similar to our approach. However, UT-PCRII takes advantage of the V-shape wheels to avoid unwanted horizontal rolling while Pobot V2[1] uses a mechanism to control such rotations. Furthermore, UT-PCRII incorporates the active spring leg (SL) mechanism to increase the stability of the robot.

[1] It should be mentioned that the initial design of UT-PCRII was reported in CLAWAR 2008 and Pobot V2 was reported in CLAWAR 2009.

3. Robot Specification

The robot consists of two arms: (a) the strap arm (SA), which is analogous to the human climber's strap, and (b) the SL (Fig. 2a). A hinge connects the SL into the SA, and a spring attached between the two to provide further stability in descending poles, especially when the pole has a step. Also, the SL ensures that the robot would stick to the pole in case a free fall happens.[2] Although the SL provides extra stability and features for this human-inspired robot, the robot can fully function, i.e., climb poles and descend poles, without the spring leg. The SA has two wheels: one is an active wheel with rubber coating, which provides adequate friction for stably climbing and descending a pole. The other wheel is a free wheel, made of Teflon, which allows the SA to adjust the robot during climb and descend. The active wheel is connected to a motor through a worm gearbox, which locks the active wheel when the motor is not powered. This is an important feature, which does not let the robot fall if the motor or power failure occur. Fig. 2(b) shows the sizes of the full-scale implementation on an actual street light pole.

4. Static Analysis

In this section, we provide the analysis of the robot. As in other wheel-based mobile robot cases, it is assumed that the robot moves slowly such that the quasi-static condition is held and the static forces are dominant. The following notations are used throughout this analysis:

- F_s : Spring force,
- F_f : Friction force between active wheel and the pole,
- w_1 : Body weight (weight of the robot excluding the spring leg),
- w_{SL} : Weight of the spring leg.

Also, the robot excluding the SL and the spring is called the robot base throughout this paper. Also, for easier presentation, the angle between the center of gravity of the

[2] Free fall may happen at the initial step when the robot is positioned to climb a pole or if a hard shake is applied to the pole resulting to temporary detachment of the robot from the pole.

https://doi.org/10.1017/S0263574711000579 Published online by Cambridge University Press

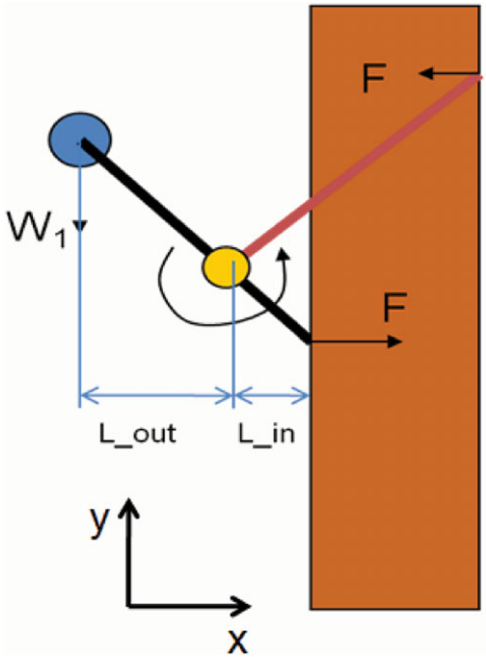


Fig. 3. (Colour online) The schematic of the mechanism attached to a pole and the effective forces. Since the radius of the active wheel, which is equivalent to L-in, is greatly smaller than L-out, it can be ignored in the analysis.

base of the robot, on which w_1 is applied, and the x-direction is assumed to be zero. In reality, there would be an angle, depending on the diameter of the pole, and the torque created by w_1 should be multiplied by the cosine of that angle. Finally, as it shown in Fig. 3, the point of attachment of the SA to the robot base in somewhat, i.e., equivalent to L-in in Fig. 3, away from the point of the contact of the robot with the pole. However, since in actual implementation, L-in, i.e., the radius of the active wheel, is far smaller than L-out, it can be ignored, and it is ignored in the following analysis.

4.1. Stability analysis

Figure 4 shows the robot's side view and the forces applied on the robot. By writing the force equilibrium equations at the SL (Fig. 4c), it can be shown that

$$F_3 - F_s \cos(\gamma) - F_{Sl_x} = 0, \tag{1}$$

in which F_{Sl} is the force applied at the SL at the hinge point (marked as H). Similarly, the forces in the y-direction should be neutralized

$$F_{SL_y} + F_s \sin(\gamma) - w_{SL} = 0, \tag{2}$$

and finally, the torque should be zero resulting into

$$F_s \times HI \sin(\beta - \gamma) - w_{SL} \times \frac{l_2}{2} \cos(\beta) - F_3 \times l_2 \sin(\beta) = 0. \tag{3}$$

Since w_{SL} is negligible compared to the spring force and the weight of the robot base,[3] by combining Eqs. (1) and (3), the force applied at the hinge in the x-direction, i.e., F_{SL_x} can be calculated

$$F_{SL_x} = F_s \times \left(\frac{HI \sin(\beta - \gamma)}{l_2 \sin(\beta)} - \cos(\gamma) \right). \tag{4}$$

If the spring is attached to the middle of the spring leg, then the above equation can be simplified to

$$F_{SL_x} = -F_s \times \left(\frac{\sin(\beta - \gamma)}{2 \sin(\beta)} \right). \tag{5}$$

Now, the equations for equilibrium in directions x and y at W (i.e., active wheel point) should be zero, which results into

$$F_1 = F_s \times \left(\frac{\sin(\beta - \gamma)}{2 \sin(\beta)} \right) + F_2, \tag{6}$$

$$F_f - F_{SL_y} - F_s \sin(\gamma) - w_1 = 0. \tag{7}$$

By substituting F_{SL_y}, F_f is calculated and F_2 can be calculated based on μ_k from Eq. (6):

$$F_2 = -\frac{w_1}{\mu_k} - F_s \times \left(\frac{\sin(\beta - \gamma)}{2 \sin(\beta)} \right). \tag{8}$$

Finally, the total torque should be zero and F_2 can be calculated

$$F_2 \times l_1 \sin(\alpha) - F_{SL_x} \times HW_y - F_{SL_y} \times HW_x - F_S \times SW_x \sin(\gamma) - F_S \times SW_y \cos(\gamma) - w_1 \times CW_x = 0. \tag{9}$$

Then, μ_k, the friction of coefficient needed to stabilize the robot, can be calculated based on the robot characteristics using Eqs. (8) and (9)

$$\mu_k = \frac{w_1}{F_2 - F_s \times \left(\frac{\sin(\beta - \gamma)}{2 \sin(\beta)} \right)}. \tag{10}$$

As it was mentioned earlier, the SL is added to provide further stability for the robot. Thus, if we show that the robot is stable without the spring leg, it should be stable with the SL for sure. If we assume that the SL is not attached, then $F_s = 0$ and μ_k is equal to

$$\mu_k = \frac{l_2 \sin(\alpha)}{CW_x}. \tag{11}$$

Equation (11) shows that the robot is stable as long as μ_k is greater than the above value, i.e.,

$$\mu_k \geq \frac{l_2 \sin(\alpha)}{CW_x}. \tag{12}$$

This is a unique characteristic of this robot, i.e., the robot is stable regardless of its weight as long as the center of the gravity of the robot is far enough from the pole on the active wheel side. In other words, if the payload is very high, still the robot is naturally stable in contrast to the traditional pole climber robots, which have limited payload. However,

[3] This assumption is true since the weight attached to the robot base is more than 20 times bigger than the weight of spring leg. Nonetheless, it can be easily included in the calculation.

https://doi.org/10.1017/S0263574711000579 Published online by Cambridge University Press

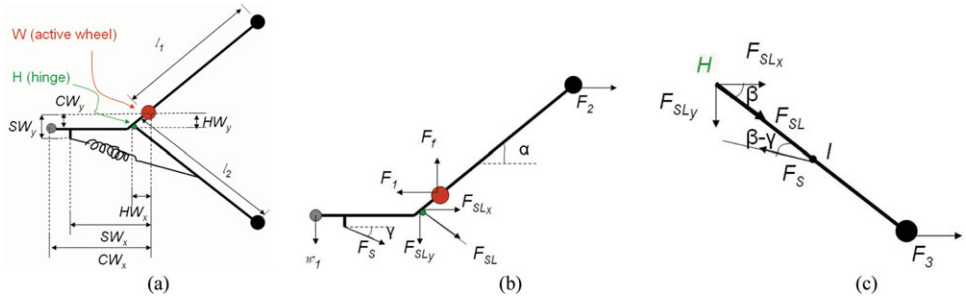


Fig. 4. (Colour online) (a) the schematics of the robot showing the distances (b) the forces applied on the base of the robot and (c) the forces on the SL.

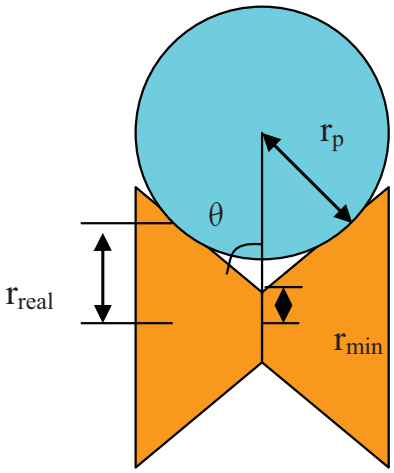


Fig. 5. (Color online) The top view of the pole (green) and the V-shape wheel. The real radius of the active wheel depends on the radius of the pole in contact.

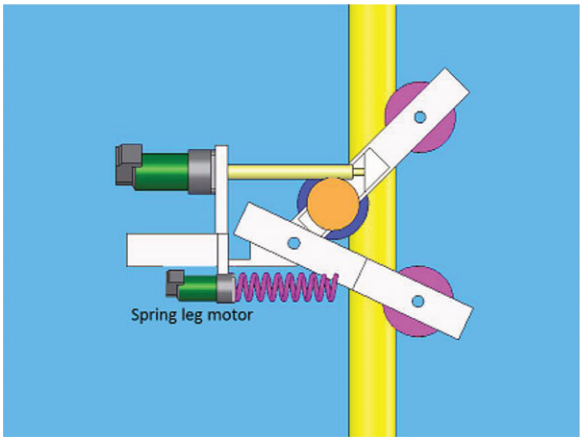


Fig. 6. (Colour online) The spring tension motor used to change the tension on the spring to adjust based on a pole's diameter.

it brings a restriction on the distribution of the payload. In other words, the center of gravity for the whole robot, the robot plus its payload, should remain away from the pole on the active wheel side. Thus, if a mechanical arm is attached to the robot, for washing, cleaning, or maintenance, then the robot should be designed in a way that the motion of the arm would not move the center of gravity toward the pole more than the allowed amount. It is clear that the allowable increase in the payload is limited to the mechanical strength of wheels such that the wheels are not deformed and can roll easily on the pole.

It is important to note that $\sin(\alpha)$ depends on the radius of the pole, as shown in the following equation, in which r_p is the radius of the pole:

$$\sin(\alpha) = \sqrt{1 - \cos^2(\alpha)} = \sqrt{1 - \frac{4r_p^2}{l_2^2}}. \tag{13}$$

In other words, if the pole's diameter is big, $l_2 \sin(\alpha)$ becomes smaller and smaller μ_k can make the robot stable. On the other hand, if the pole's diameter is small, $l_2 \sin(\alpha)$ becomes bigger and bigger coefficient of friction is needed (Eq. 14)

$$l_2 \sin(\alpha) = \sqrt{l_2^2 - 4r_p^2}. \tag{14}$$

This is important in the design of the robot since in practice, the telephone or light poles have bigger diameter in the bottom of the pole and smaller diameter at the top. Thus, the robot should be designed for the top of the pole to satisfy the stability criterion.

4.2. The real radius of the active wheel

Since the active wheel has a V-shape structure, its actual radius, i.e., the radius that is in contact with the pole, depends on the diameter of the pole (Fig. 5). The real radius can be calculated based on the angle of the V-shape wheel, the minimum radius of the active wheel, and the radius of the pole at the contact point

$$r_{real} = \frac{r_p \cos^2(\theta)}{\sin(\theta)} + r_{\min}. \tag{15}$$

It should also be noted that with a given weight and spring tension, the maximum force on the contact points of the active wheel with a pole can be applied when θ is 45°.

5. Simulation and Experiments

Figure 6 shows the schematic of the pole climber, including the spring motor, which can stretch the spring to increase effect of the spring wheel on the pole. The SL motor is currently controlled by the operator. When the robot moves from high-diameter parts of a pole to low-diameter section, the operator activates the motor, which simply pulls the spring toward itself. Consequently, the lower free wheel is pushed harder to the pole providing further stability due to

https://doi.org/10.1017/S0263574711000579 Published online by Cambridge University Press

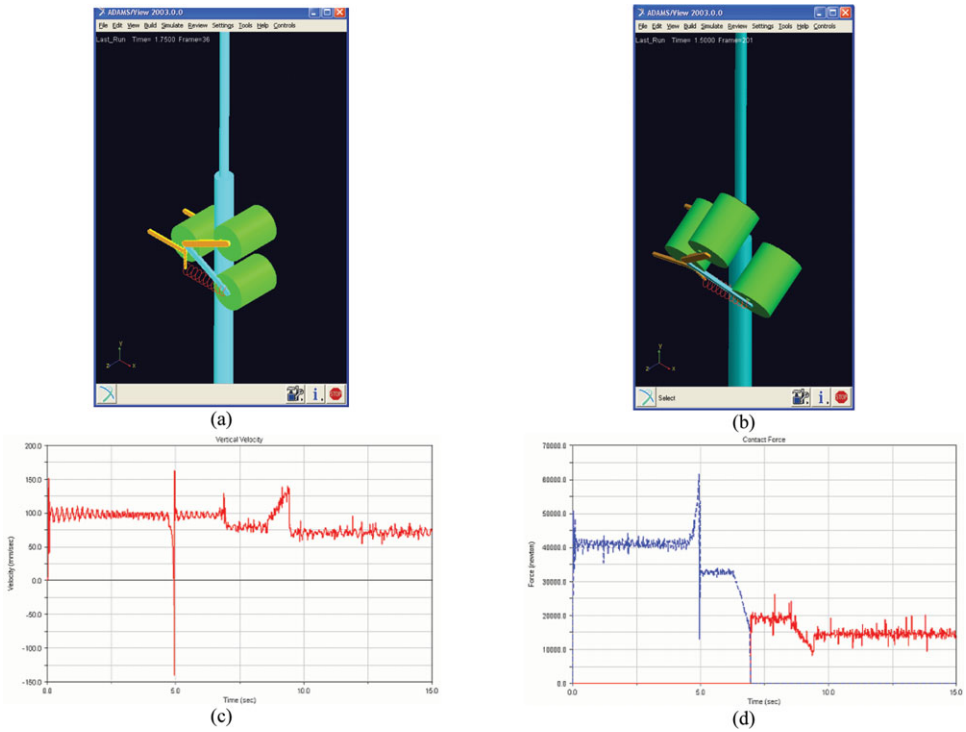


Fig. 7. (Color online) The simulation of the robot in ADAMS. (a) the robot modeled on a pole with two levels, (b) the robot, with cylindrical wheels, may detach itself and fall due to noise or disturbances when the spring stiffness is low. (c) the velocity of the robot along the path. (d) the force applied to the pole by the active wheel. The blue curve shows the force on the lower level of the pole and the red one shows the force on the upper level of the pole.

the increased friction force between the active wheel and the pole. In contrast, when the robot descends the pole, i.e., going from low-diameter section to a high-diameter section, the motor reduces the tension on the spring, which makes the robot to descend easier. In future models, the control of the SL motor can be done automatically using the angle of the SL with the pole.

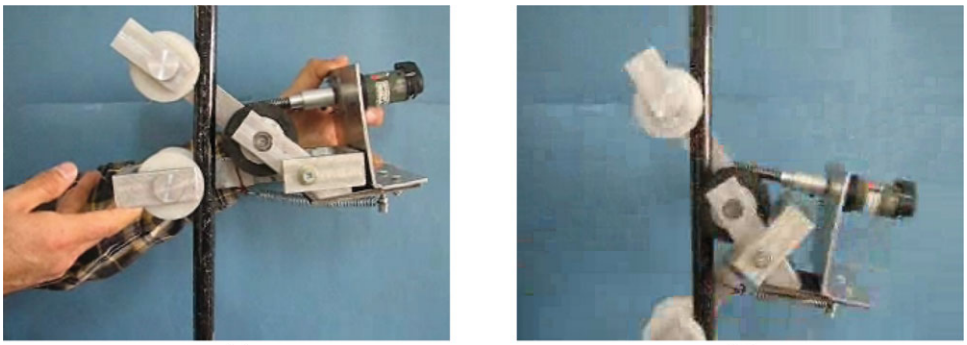
Figure 7 shows the simulation of the robot in ADAMS. The robot was simulated with cylindrical wheels, with 100 mm radius, rather than V-shape wheels for the sake of simplicity at the current stage of our research. The spring has 100 N/mm stiffness and 100 mm length at no load. The initial length of the spring, i.e., at the bottom of the pole, is 300 mm that provides enough contact force for stable climb and descend. The simulated pole has 1500 mm length with two levels, Level 1 with 50 mm radius and Level 2 with 25 mm radius. In this simulation, there is no weight attached to the back of the robot to study the impact of the spring in the stability of the robot. Consequently, the robot would slip if the spring stiffness falls below 3 N/mm. At 30 N/mm, the robot could climb the first level of the pole, i.e., the 50 mm diameter level, but started slipping on the second level. Figure 7(b) shows the case that the spring stiffness is not enough to hold the robot to the pole. Consequently, slight disturbance, which happens at the transition between two levels of the pole, makes the robot to detach itself from the pole. This shows the importance of V-shape wheels to compensate the noise and disturbances. It is also important to mention that increasing the spring stiffness would allow the robot to overcome small disturbances and stay attached to the pole. Figure 7(c) shows the vertical velocity of the robot, which stays constant along the pole except at the change of pole diameter. The velocity stays around nominal 100 mm/s and only changes when the robot passes through the step between the two levels of the pole. Figure 7(d) shows the force applied on the pole by the active wheel. The force reduces when the robot moves to the second level of the pole since the length of the spring is reduced. Since the spring is less stretched on the second level of the pole, it applies less force on the pole. That is why, a mechanism implemented to ensure that adequate force is applied all over the pole.

Two versions of the robot have been actually built; a small version weighing about 2 Kg, and a full-scale version weighing about 25 Kg.[4] The small version was tested carrying a 10 Kg weight showing that it can carry more than five times of its weight. Furthermore, a series of test were conducted to test the impact of weight on the climbing time. Table I shows the climbing time for a series of the weights along 25 cm length of a pole for an active wheel with 2.3 cm radius (at the bottom part of a three-level pole) and 5 rotations/min. The result shows slight increase in the time while the weight is increased 10 times.

Another test was conducted to determine the speed of the robot on poles with different diameters (on the three-level pole). The speed of the robot on a 30 mm level was 10 mm/s while it was 8.7 mm/s on the 20 mm level. This drop in the speed is due to the change in the real diameter of the active wheel. In other words, since the pole is smaller, the real radius of the active wheel has reduced resulting in reduction in speed. The robot was also tested against free fall and showed its ability to stabilize shortly after a free fall (Fig. 8).

[4] This is the weight for the first prototype. Our second prototype would weight about half of this, i.e. 13 Kg.

https://doi.org/10.1017/S0263574711000579 Published online by Cambridge University Press



(a) (b)

Fig. 8. (Colour online) The free fall test. (a) The robot is held in the mid air without contacting the poll, (b) the robot is attached to the pole after being released in the mid air. First the SL contacts the pole and then the spring drags the active wheel toward the pole creating adequate contact for stable grasp to the pole.

Table I. Climbing time.

#	Weight (Kg)	Climbing time (s)
1	0.5	22.00
2	1.0	22.32
3	2.0	22.98
4	3.0	24.25
5	4.0	24.69
6	5.0	25.44

Figure 9(a) shows the full-scale implementation of the robot while a person holds on to it. A gradual climbing on a light pole is shown in Figs. 9(b)–9(d). The light pole is 8 m tall and has 13, 11, and 9 cm diameter at lower, middle, and top part of it, respectively. In this prototype, a SL motor is used to allow changing the length of the spring in case more tension is needed. This allows the robot to climb very slim poles, which especially happens at the top of poles.

Figure 10 shows the washing mechanism attached to the climbing robot to wash the lamps. A water jet is used to wash the lamp using high-pressure water. The results show that this mechanism would be effective if the water jet gets close enough, i.e., 30 cm or closer, to the lamp. Otherwise, it would not clean very dirty, and especially oily, lamps. A wireless camera is mounted on the water



(a) (b) (c) (d)

Fig. 9. (Colour online) The actual implementation. (a) The full size robot is stable even when a person holds on to it, (b) the start of climbing position, (c) at the middle of the pole, and (d) at the top of the pole. The robot could easily pass the leaves and other small obstacles on its path.

https://doi.org/10.1017/S0263574711000579 Published online by Cambridge University Press



(a) (b)

Fig. 10. (Colour online) Water jet washing mechanism: (a) the camera view of the water jet washing mechanism, which provides close view for aiming at the lamp and the cleaning progress and (b) a view of the washing process. The water jet (lower left corner of the image) shoots the water from a meter away from the lamp.

jet to allow clear look at the lamp and proper zooming on it.

6. Discussion

In this paper, we present a human-inspired pole climbing robot that has been successfully designed, implemented, and tested. The robot has an exceptional characteristic, which makes it unique among the climbing robots, i.e., it is naturally stable. Moreover, the bigger the load on the robot, the better its stability. This wheel-based design provides continuous and fast motion, which is advantageous compared to other nonwheel-based robots. Finally, it has a simple design, a light structure, and very simple control mechanism.

In future work, we will formulate the dynamics of this robot and will explore the use of tracks instead of wheels. We will also investigate on the methods and designs that will allow the robot to climb poles that have extensions at the middle. Finally, further safety and stability features, such as magnets on the active wheel, would be added to the robot.

Acknowledgments

This research is financially supported in part by the Iranian Electrical Power Generation, Distribution, and Transmission Company (TAVANIR Co.). The authors wish to thank Mr. Gh. Rajabi of TAVANIR Co. for the fruitful discussions. The authors like to thank Mr. Ehsan Noohi for his help on simulating the robot and Mr. Nader-Ali for his help in testing the robot. The authors also like to thank Ms. Leila Kashani for her feedback on the paper.

References

1. V. Krasnoslobodtsev and R. Langevin, "Triz Application in Development of Climbing Robots," *First TRIZ Symposium,* Japan (Sep. 2005).
2. H. Zhang, J. Zhang and G. Zong, "Effective pneumatic scheme and control strategy of a climbing robot for class wall cleaning on high-rise building," *Int. J. Adv. Robot. Syst.* **3**(2), 183–190 2006.
3. C. Menon and M. Sitti, "A biomimetic climbing robot based on the gecko," *J. Biomic Eng.* **3**, 115–125 (2006).
4. A. Baghani, M. Nili Ahmadabadi and A. Harati, "Kinematics Modeling of Wheel-Based Pole Climbing Robot (UT-PCR)," *Proceedings of the International Conference on Robotics and Intelligent Systems*, Beijing, China (2006) pp. 5007–5012.
5. T. White, N. Hewer, B. Luk and J. Hazel "The Design and Operational Performance of a Climbing Robot Used for Weld Inspection in Hazardous Environments," *Proceedings of the IEEE International Conference on Control Applications*, Trieste, Italy (Sep. 1–4, 1998) pp. 451–455.
6. B. Luk, D. Cooke, S. Galt, A. Collie and S. Chen, "Intelligent legged climbing service robot for remote maintenance applications in hazardous environments," *Int. J. Robot. Auton. Syst.* **53**(2), 142–152 (2005).
7. M. Tavakoli, M. R. Zakerzadeh, G. R. Vossughi and S. Bagheri, "Design and Prototyping of a Hybrid Pole Climbing and Manipulating Robot with Minimum DOFs for Construction and Service Applications," *Proceedings of the Climbing and Walking Robots (CLAWAR)*, Madrid, Spain (2004) pp. 1071–1076.
8. A. Degani, H. Choset and M. T. Mason, "DSAC—Dynamic, Single Actuated Climber. Local Stability and Bifurcations," *Proceedings of the IEEE International Conference on Robotics and Automation*, Anchorage, AK (2010) pp. 2803–2809.
9. M. Abderrahim, C. Balaguer, A. Gimenez, J. M. Pastor and V.M. Padron, "ROMA: A Climbing Robot for Inspection Operations," *Proceedings of the IEEE International Conference on Robotics and Automation*, Detroit, Michigan (1999) pp. 2303–2308.
10. F. Bonaccorso, C. Bruno, D. Longo and G. Muscato, "Structure and Model Identification of a VORTEX-Based Suction Cup," *Proceedings of the 11th International Conference on Climbing and Walking Robots and the Support Technologies for Mobile Machines*, Coimbra, Portugal (Sep. 8–10, 2008) pp. 303–310.
11. G. C. Haynes, A. Khripin, G. Lynch, J. Amory, A. Saunders, A. Rizzi and D. E. Koditschek, "Rapid Pole Climbing with a Quadrupedal Robot," *Proceedings of the IEEE International Conference on Robotics and Automation*, Kobe, Japan (May 2009) pp. 2767–2772.
12. C. Balaguer, A. Gimenes, J. Pastor, V. Padron and C. Abderrahim,"A climbing autonomous robot for inspection application in 3D complex environments," *Robotica* **18**(3), 287–297 (2000).
13. Z. Xu and P. Ma, "A wall-climbing robot for labeling scale of oil tank's volume," *Robotica* **20**(2), 203–207 (2002).
14. G. La Rosa, M. Messina, G. Muscato and R. Sinatra, "A low cost lightweight climbing robot for the inspection of vertical surfaces," *Mechatronics* **12**(1), 71–96 (2002).
15. R. Lal Tummala, R. Mukherjee, N. Xi, D. Aslam, H. Dulimarta, J. Xiao, M. Minor and G. Dang, "Climbing the walls," *IEEE Robot. Autom. Mag.* **9**(4), 10–19 (2002).

https://doi.org/10.1017/S0263574711000579 Published online by Cambridge University Press

16. J. Zhu, D. Sun and S. Tso, "Development of a tracked climbing robot," *J. Intell. Robot. Syst.* **35**(4), 427–444 (2002).
17. T. Bretl, "Motion planning of multi-limbed robots subject to equilibrium constraints: The free-climbing robot problem," *Int. J.Robot. Res.* **25**(4), 317–342 (2006).
18. B. Kennedy, A. Okon, H. Aghazarian, M. Badescu, X. Bao, Y. Barcohen, Z. Chang, B. Dabiri, M. Garrett, L. Magnone and S. Sherrit, "Lemur iib: A Robotic System for Steep Terrain Access," *Proceedings of the 8th International Conference on Climbing and Walking Robots*, London, UK (2005).
19. K. Lipkin, I. Brown, A. Peck, H. Choset, J. Rembisz, P. Gianfortoni and A. Naaktgeboren, "Differentiable and Piecewise Differentiable Gaits for Snake Robots," *Proceedings of the IEEE/RSJ International Conference of Intelligent Robots and Systems*, San Diego, CA (Nov. 2007) pp. 1864–1869.
20. J. McKenna, D. Anhalt, F. Bronson, H. Brown, M. Schwerin, E. Shammas and H. Choset, "Toroidal Skin Drive for Snake Robot Locomotion," *Proceedings of the IEEE International Conference on Robotics and Automation*, Pasadena, CA (May 2008).
21. J. C. Fauroux and J. Morillon, "Design of a climbing robot for cylindro-conic poles based on rolling self-locking," *Ind. Robot-An Int. J.* **37**(3), 297–292 (2010).

https://doi.org/10.1017/S0263574711000579 Published online by Cambridge University Press